Journal Pre-proof

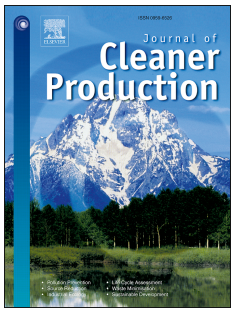

Bismuth phosphinate incorporated nanocellulose sheets with antimicrobial and barrier properties for packaging applications

Maisha Maliha, Megan Herdman, Rajini Brammananth, Michael McDonald, Ross Coppel, Melissa Werrett, Philip Andrews, Warren Batchelor

PII: S0959-6526(19)33886-7

DOI: https://doi.org/10.1016/j.jclepro.2019.119016

Reference: JCLP 119016

To appear in: *Journal of Cleaner Production*

Received Date: 11 April 2019

Revised Date: 16 September 2019

Accepted Date: 22 October 2019

Please cite this article as: Maliha M, Herdman M, Brammananth R, McDonald M, Coppel R, Werrett M, Andrews P, Batchelor W, Bismuth phosphinate incorporated nanocellulose sheets with antimicrobial and barrier properties for packaging applications, *Journal of Cleaner Production* (2019), doi: https://doi.org/10.1016/j.jclepro.2019.119016.

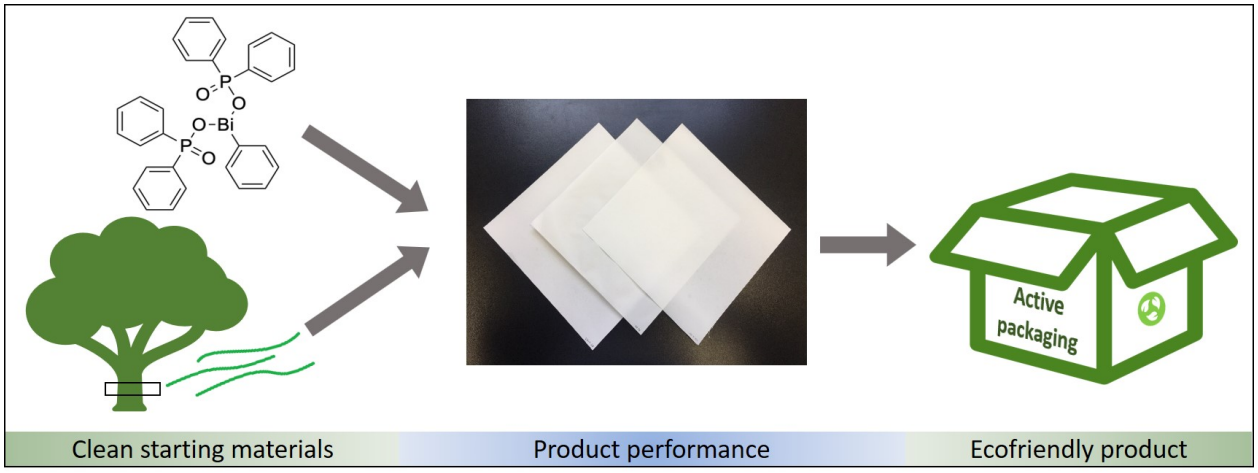

Bismuth phosphinate incorporated nanocellulose sheets with antimicrobial and barrier properties for packaging applications

Maisha Maliha[1], Megan Herdman[2], Rajini Brammananth[3], Michael McDonald[4], Ross Coppel[3], Melissa Werrett[2], Philip Andrews[2], Warren Batchelor[1]

[1]*Bioresource Processing Research Institute of Australia (BioPRIA), Department of Chemical Engineering, Monash University, VIC 3800, Australia*

[2]*School of Chemistry, Monash University, VIC 3800, Australia*

[3]*Department of Microbiology, Monash University, VIC 3800, Australia*

[4]*Centre for Geometric Biology, School of Biological Sciences, Monash University, VIC 3800, Australia*

Corresponding author email: warren.batchelor@monash.edu

Highlights

- Nanocellulose composites with varying bismuth complex content were developed.
- The physical, mechanical and barrier properties against water vapor were studied.
- Bismuth complex has little effect on barrier property unless present at high level.
- Composites can inhibit the growth of medically important bacteria and fungi.
- Composite are more effective on Gram-positive bacteria, even at very low loading.

Abstract

The incorporation of an organobismuth complex into a nanocellulose matrix to develop a free-standing antimicrobial barrier material was investigated. The non-toxic complex, phenyl bismuth *bis*(diphenylphosphinato) was used as the additive to impart antimicrobial properties to nanocellulose sheets for the development of paper-based renewable and biodegradable active packaging material. A spraying technique was used to prepare sheets with different loadings of the organobismuth complex and its effects on antimicrobial and barrier properties were studied. Morphological studies of the sheets revealed the overall distribution of the complex throughout the nanocellulose matrix, with occasional clustering behaviour on the surface. Water vapour permeability of the paper sheets increased very slightly with loading of the bismuth complex, but remained in the range acceptable for packaging materials. The physical and mechanical properties of the sheets were also affected by the addition of the bismuth complex in the structure, and hence a trade-off needs to be made between the loading level and the material performance for commercialization. The composite sheets were able to inhibit the growth of bacteria and fungi, including strains of multidrug resistant bacteria. Moreover, the paper showed continued release of the bismuth complex over time with effective lifetime depending on the loading. In summary, this paper describes the preparation and characterization of a sustainable and ecofriendly antimicrobial composite paper, using a poorly soluble bismuth complex dispersed into nanocellulose matrix, which shows the potential to be used as an active packaging material.

Keywords: nanocellulose, bismuth, antimicrobial, packaging, barrier

1. Introduction

Packaging plays a vital role for most products in terms of consumer safety. Conventional packaging serves only as a barrier layer between the product and the environment and shields it from oxygen, water vapour and other contaminants (Pereira De Abreu, Cruz et al. 2012). Demand for quality assurance and product safety of sensitive items such as food and medical products has led to the emergence of high-value active packaging material that offers enhanced protection (Lavoine, Desloges et al. 2015, Inamuddin 2016). Active packaging has the ability to either interact with the product or alter the environment enclosed within the packaging. Examples include incorporating compounds that can absorb and remove oxygen, ethylene or moisture, or have antimicrobial properties [1]. The latter offers better protection by inhibiting the microbial contamination of the products reducing the risk of deterioration. It can also inhibit contamination of the packaging surface, thus reducing microbial cross-contamination from the packaging. This is an effective strategy with proven improvements in product protection and quality (Appendini and Hotchkiss 2002, Pereira De Abreu, Cruz et al. 2012). Antimicrobial active packaging can be obtained by incorporating or immobilizing antibacterial and antifungal agents into the material (Lavoine, Desloges et al. 2015, Amini, Azadfallah et al. 2016, Lavoine, Guillard et al. 2016).

The use of metal-based antimicrobial agents, in the form of nanoparticles and compounds, has been increasing (Patra, Gasser et al. 2012, Barry and Sadler 2013, Dizaj, Lotfipour et al. 2014). This is due to metals often showing greater efficacy and resilience to bacterial resistance than the organic compounds. (Lemire, Harrison et al. 2013). Metals such as silver, gold, arsenic, bismuth, antimony, copper, mercury, platinum, palladium, ruthenium, and cobalt, and their compounds have shown antimicrobial activity (Abd-El-Aziz, Agatemor et al. 2017, Alvarez-Paino, Munoz-Bonilla et al. 2017). This includes inorganic compounds, organometallic complexes, metal organic frameworks and metal nanoparticles (Patra, Gasser et al. 2012, Barry and Sadler 2013, Abd-El-Aziz, Agatemor et al. 2017). Of them, silver has been the most popular metal used as an antimicrobial additive in materials (Dankovich and Gray 2011, Haider and Kang 2015, Huang, Li et al. 2015, Amini, Azadfallah et al. 2016, Carbone, Donia et al. 2016, Xiong, Zhu et al. 2016). Silver nanoparticles have been studied as composites with synthetic and natural polymers, such as cellulose, chitosan, gelatine, chitin, and collagen (Martínez-Abad, Lagaron et al. 2012, Xiong, Zhu et al. 2016, Yan, Abdelgawad et al. 2016). Silver is also used in various commercial products, including packaging materials, clothing, and healthcare and personal care products. This widespread use of silver has raised concerns about its toxicity for various organisms including humans and environmental accumulation (Barros-Velázquez , Stensberg, Wei et al. 2011, Cushen, Kerry et al. 2012). The most severe toxic effect of long-term silver exposure to humans is the condition of blue coloration of the skin, known as argyria. Other harmful effects of soluble silver include damage to liver, kidney and blood cells (Drake and Hazelwood 2005, Maillard and Hartemann 2013). Silver nanoparticles can enter the human body

through gastrointestinal absorption from food contact materials (e.g. silver based food-packaging) as well as through the respiratory tract (Cushen, Kerry et al. 2012). The maximum safe level of lifetime silver intake is only 10g as declared by the World Health Organization (Cao 2017). Studies have shown that silver nanoparticles can migrate into food from silver-based food-packaging materials (Huang, Chen et al. 2011, Echegoyen and Nerín 2013). It has also been reported that the concentration of silver released into food from a commercial packaging material can exceed the regulatory limits set for food contact materials after 24 days of storage (Pezzuto, Losasso et al. 2015). This suggests there is a necessity to develop new active packaging materials, with more attention to safety and health concerns. In addition, the prolonged use of silver has raised the risk of induction of silver resistance in bacteria (Silver 2003, Maillard and Hartemann 2013, Gunawan, Marquis et al. 2017), a scenario common for many other metal-based antimicrobials (Pal, Bengtsson-Palme et al. 2014). As a result, it has been suggested that silver-based antimicrobials be regulated by governments and reserved for medical uses only (Crocetti 2013). Accordingly, there is a need for a new generation of antimicrobial compounds for use in active packaging for food, medical supplies and other sensitive products.

The purpose of this study is to investigate a poorly soluble bismuth complex as an active species for packaging applications. Many bismuth complexes have been reported to possess antibacterial activity (Domenico, Baldassarri et al. 2001, Kotani, Nagai et al. 2005, Svoboda, Jambor et al. 2010, Luqman, Blair et al. 2016, Andrews, Werrett et al. 2018). Bismuth has a long history of being used for treating intestinal disorders: Pepto-Bismol (BSS or bismuth subsalicylate) and De-Nol (CBS or colloidal bismuth subcitrate) are used as gastrointestinal treatments, for example traveller's diarrhoea, and are effective agents against the bacteria *Helicobacter pylori* (Briand and Burford 1999, Suzuki and Matano 2001, Barry and Sadler 2013). It is proposed that bismuth works by binding to proteins with metal binding sites, e.g. thiol (cysteine) rich protein structures (Keogan and Griffith 2014). Unlike other heavy metals, bismuth displays a low level of toxicity in humans and is non-carcinogenic (Kotani, Nagai et al. 2005). Although it is a heavy metal in the pnictide (Gp 15) family, where toxicity is assumed to increase with molecular weight, bismuth is unique in its comparatively low-toxicity (Suzuki and Matano 2001). In this paper, a new class of organobismuth complex, phenyl bismuth *bis*(diphenylphosphinato), has been chosen as the active agent. This has been reported to have little or no toxicity to mammalian cells and has significantly low solubility in water (Andrews, Werrett et al. 2018). As a result, in the context of packaging, the risks of migration into the product or into the environment is also greatly reduced.

The technical challenge for applications in active packaging lies in the choice of material that is suitable for use in supporting the antimicrobial agents. In this regard, polymers have been widely used as the carrier matrix for antimicrobial agents to improve their stability and activity due to their macromolecular properties (Alvarez-Paino, Munoz-Bonilla et al. 2017). The most studied materials

for antimicrobial films are petroleum based polymers, e.g. polyethylene, polypropylene, polystyrene and polyethylene terephthalate (Martínez-Abad, Lagaron et al. 2012, Alvarez-Paino, Munoz-Bonilla et al. 2017). The packaging industry is also mainly dependant on petroleum-based polymers (Inamuddin 2016). Environmental accumulation of plastics, and the resulting impact from plastic pollution, have driven interest in the use of biodegradable polymers such as polylactic acid (PLA), polyglycolic acid (PGA), and more importantly renewable natural biopolymers such as cellulose, starch, chitosan, alginate, and collagen (Alvarez-Paino, Munoz-Bonilla et al. 2017). Of them, cellulose is the most abundant, biodegradable and renewable, as well as inexpensive and non-toxic (O'Sullivan 1997, Xu, Chen et al. 2016). However, while cellulose fibres can be formed into strong and stiff paper-based packaging, the barrier properties are inferior to that of petroleum-based polymers. This limitation can be overcome by breaking down cellulose-containing materials into microfibrils or bundles of microfibrils. The product, which is generally known as nanocellulose, has excellent strength and greatly improved barrier properties when compared to conventional paper (Siró and Plackett 2010, Lavoine, Desloges et al. 2012, Kumar, Bollström et al. 2014). Nanocellulose is unique due to its hydrophilicity, biocompatibility and large surface area in addition to all the attributes of nanostructured materials (Klemm, Heublein et al. 2005, Klemm, Kramer et al. 2011). Nanocellulose films also provide a porous structure for antimicrobial agents to attach to, both physically and chemically (Lin and Dufresne 2014), making nanocellulose a promising material for active packaging applications. Nanocellulose suspensions can be converted to sheets and films by various methods such as vacuum filtration (Varanasi and Batchelor 2013), casting (Kumar, Bollström et al. 2014), spraying (Beneventi, Chaussy et al. 2014, Krol, Beneventi et al. 2015, Beneventi, Zeno et al. 2016) or coated on a substrate /base paper (Lavoine, Desloges et al. 2015, Kumar, Koppolu et al. 2017).

The objective of this study was to incorporate a new class of organobismuth complex, phenyl bismuth *bis*(diphenylphosphinato), into a nanocellulose matrix for the development of cleaner antimicrobial sheets for active packaging applications. Antimicrobial performance, physical, mechanical and barrier properties of the free-standing nanocellulose paper sheets were thoroughly studied to demonstrate the hypothesis that these materials can potentially serve as an active barrier layer as a standalone sheet or as coatings on other materials.

2. Materials and Method

2.1. Materials

Microfibrillated Cellulose (MFC) purchased from DAICEL Chemical Industries Limited, Japan (grade Celish KY-100G) was used as the nanocellulose matrix. The MFC used was characterized in previous work by Varanasi *et al*. to have a mean diameter of 73 nm and an aspect ratio of 147 (Varanasi, Chiam et al. 2012). Phenyl bismuth *bis*(diphenylphosphinato) was prepared according to

Andrews *et al*. (Andrews, Werrett et al. 2018). Triphenyl bismuth and diphenyl phosphinic acid were mixed in the ratio of 1:2 in ethanol and heated at reflux for 24 hours. The reaction mixture was then filtered, and the insoluble phenyl bismuth *bis*(diphenylphosphinato) was isolated as a white powder. Following filtration, the complex was washed with hot ethanol to remove all unreacted chemicals and the by-product benzene, after which no further purification was required.

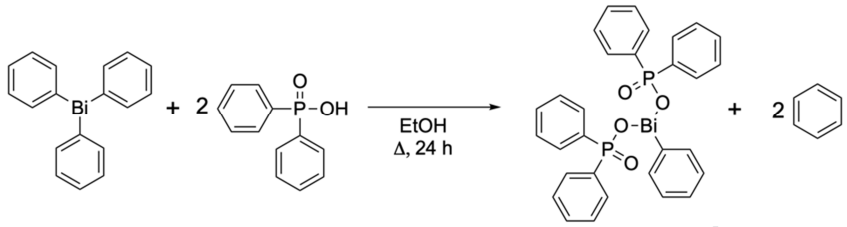

Scheme 1: Chemical reaction for the synthesis of phenyl bismuth *bis*(diphenylphosphinato)

All analytical data matches that previously reported for the phenyl bismuth bis(diphenylphosphinato) complex (as shown in Scheme 1). The complex is sparingly soluble in water and the solubility as reported is 16.3 kg of water required to dissolve 1 g complex. The complex was also previously reported to have limited solubility in organic solvents like ethanol, dichloromethane, tetrahydrofuran, toluene, and dimethyl sulfoxide (DMSO). Moreover, preliminary toxicity results has been reported previously and it was shown that the complex has no toxic effect on mammalian COS-7 cells at a concentration of 0.5 mg/mL (Andrews, Werrett et al. 2018).

2.2. MFC Suspension Preparation

Phenyl bismuth *bis*(diphenylphosphinato) was dispersed in small amounts of water using a magnetic stirrer and mixed with the MFC. This was then diluted to make a suspension of 2 wt.% MFC and mixed with a hand blender, followed by disintegration. In the disintegrator, the suspension is contained in a 3 L vessel and a small propeller running at 3000 revolutions separates the fibres from each other. The suspensions were made with varying amount of the bismuth complex. The suspensions were made with target loadings of 5, 2.5, 1.0, 0.5, and 0.1 wt.% of the bismuth complex with respect to the mass of cellulose fibres in the suspension. Thus, the composition was 2 g fibre and 0.1g, 0.05g, 0.02g, 0.01g or 0.002g of the bismuth complex in 100 grams of the 5, 2.5, 1.0, 0.5, and 0.1 wt.% suspensions respectively, the remaining being DI water. The experimental consistency of the suspensions are given in table S1 in the supplementary information. The suspensions were sprayed immediately without any time delay to ensure no settling of the particles, thus confirming uniform dispersibility in the suspensions.

2.3. Sheet preparation

Bismuth(III) phosphinato-MFC composites were prepared using a spraying technique as described by Shanmugam *et al.* (Shanmugam, Varanasi et al. 2017). The composites were made using the suspensions described with target loadings of 5, 2.5, 1.0, 0.5, and 0.1 wt.% of the bismuth. The consistency of the fibres in the suspension was kept constant throughout. The MFC suspension was

sprayed onto square stainless steel plates moving on a variable speed conveyor set at 1 ± 0.2 cm/s. The suspension was sprayed using a Professional Wagner spray system (Model number 117) at 200 bar from a height of 30 ± 1cm. A spray tip of 517 type was used. After spraying, the MFC on the plates was dried at ambient temperature of 25^{o} C under constraint at the edges until the sheets separated from the plate and started to roll off at the edges. The sheets were then peeled from the plates and stored in a controlled temperature and humidity condition maintained at 23 ^{o}C and 50 % relative humidity.

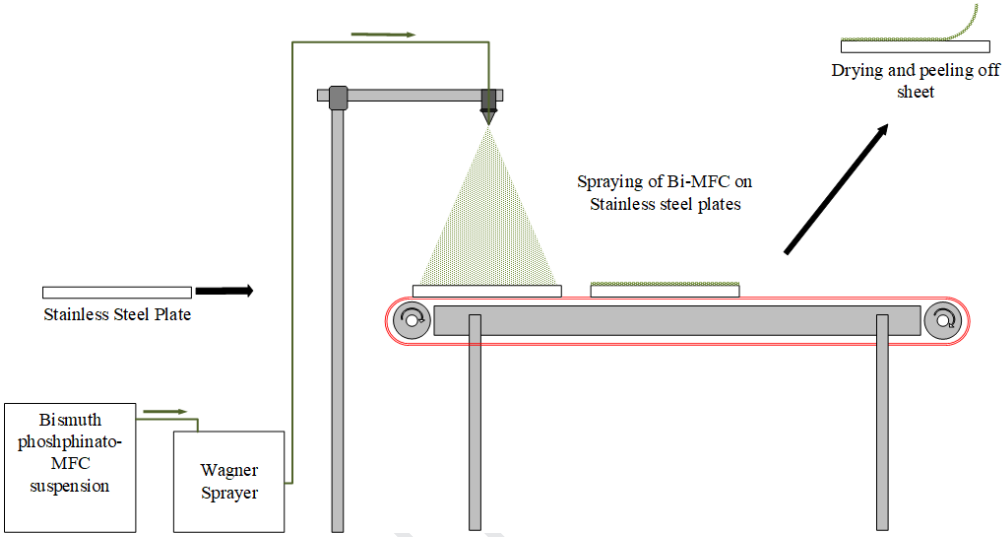

Figure 1: Experimental Setup for lab scale spraying of the bismuth (III) phosphinato-MFC suspension onto stainless steel plates

2.4. Characterization

2.4.1. ICP-OES Analysis

Weighed samples of the sheets were ashed using a muffle furnace in crucibles. During ashing, the temperature was ramped to 600 ^{o}C over three hours and maintained at this temperature for a further three hours. Above 100 ^{o}C all moisture, and at about 525 ^{o}C all cellulose, is removed. The inorganic complex decomposes at about 330 ^{o}C. The bismuth-based residue left in the crucible was dissolved in small quantities of concentrated nitric acid and diluted. This was then analysed using Perkin-Elmer Avio 200 ICP-OES (inductively coupled plasma-optical emission spectrometry). The concentration of the elemental bismuth in the sample solution was analysed by ICP-OES, and back calculated to the amount of bismuth complex in the paper. Each sheet was analysed in triplicate and reported as percentage of the mean mass of the bismuth complex per gram of dry paper ± standard deviation.

2.4.2. Bi-complex characterization

The hydrodynamic diameter of the particles was estimated using dynamic light scattering (DLS) using a Nanobrook Omni Particle Size Analyser (Brookhaven Instruments) with a dilute suspension of 0.02 wt.% Bi-complex in Milli-Q water.

2.4.3. SEM Imaging

Scanning Electron Microscope (SEM) imaging of the bismuth(III) phosphinato-MFC sheets was performed using the FEI Nova NanoSEM 450 FEG SEM and FEI Magellan 400 FEG SEM using an accelerating voltage of 5 keV and spot size 2 to study the morphology and distribution of the bismuth complex in the sheets. The samples were prepared by cutting a small piece of the composite sheet and mounting it onto a metal stub secured properly using carbon tape. The samples were coated with a thin conducting layer of Iridium metal.

2.5. Material performance

2.5.1. Antimicrobial Test

The antibacterial and antifungal activities of differently loaded bismuth(III) phosphinato-MFC sheets were measured using disk diffusion assays. The Gram-positive bacteria, viz. *Staphylococcus aureus* (*S. aureus*), *Vancomycin-resistant enterococcus* (*VRE*), and *Methicillin-resistant Staphylococcus aureus* (*MRSA*) and Gram-negative bacteria viz. *Escherichia coli* (*E. coli*) and *Pseudomonas aeruginosa* (*P. aeruginosa*) were examined. The fungi used for the tests were the non-pathogenic model organisms *Saccharomyces cerevisiae* YJM789 and *Schizosaccharomyces pombe H-*, which are known for their multidrug resistance (Kawashima, Takemoto et al. 2012), as well as the pathogenic species, *Candida albicans* SC5314 and *Candida glabrata* BG99. *C. albicans* BG99 is a pathogenic and virulent strain often used in lab and genomic studies (Hua, Yuan et al. 2009). *C. glabrata* BG99 is the lab model for the third most common cause of fungal infection in humans (Fidel, Vazquez et al. 1999). The growth media Lysogeny broth (LB) was used for the bacteria *S. aureus*, *E. coli* and *P. aeruginosa* and Brain Heart Infusion (BHI) was used for *VRE* and *MRSA*. The LB or BHI agar plates were inoculated with 100µl of the specific stationary phase bacteria. CSM plates were inoculated with 100 ml of a stationary phase overnight culture of the yeasts. The composite sheets was cut into discs of 6 mm using a standard hole punch, which were placed on the agar plate that had already been spread with the microbial culture. All strains were incubated at 37 ^{o}C for 24 hours except for *S. cerevisiae*, *S. pombe* and *C. glabrata*, which were incubated at 30 ^{o}C. For the samples that inhibited the growth of the microorganism, a clear zone was observed. The plates were then photographed and the diameter of the zone of inhibition was measured. These tests were performed in triplicate for each type of test microorganism.

2.5.2. Duration of antimicrobial action:

The 0.94 wt.% and 4.37 wt.% loaded bismuth(III) phosphinato-MFC sheets were tested to investigate the activity of the antimicrobial paper over time. The Gram-positive bacterium *Staphylococcus epidermidis* was chosen for this analysis because it is a part of human microbiota. *S. epidermidis* is the most dominant species of bacteria in human skin and mucosal surfaces, and are carried by healthy people (Fey and Olson 2010). The zone of inhibition experiment was done in the same way as for the

other bacterial strains. After 24 hours, the discs were transferred aseptically to a new fresh agar plate inoculated with the same bacterial strain and incubated for another 24 hours. This was repeated until no visible zone of inhibition was observed. Furthermore, the agar around the disks in each of these plates were analysed for presence of any bismuth in there. This was done by scooping out some agar samples, dissolving it in nitric acid and then analysing the bismuth concentration by ICP-OES.

2.5.3. Physical and mechanical properties

The mass of the sheets per unit area was measured by drying the sheet in an oven at 105^{o}C to determine the grammage. The tensile index and Young's Modulus were measured using an Instron tensile tester (model 5965). The papers were cut into15 mm width strips and conditioned before the test at 23^{o}C and 50% relative humidity for 24 hours. The span tested was 50 mm with a constant strain rate of 10mm/min. Five replicated were measured for each test. The pore size distribution and porosity were determined by mercury porosimetry using Micromeritics Autopore IV. The sheets were cut into 8 mm squares and degassed for 24 hours at 100^{o}C in the sample holder. The measurements were done in a penetrometer (Model 14, 3cc). The surface area and pore shape were determined by physisorption of nitrogen gas at 77K using a Micromeritics 3Flex.

2.5.4. Water vapor permeability

The water vapour transmission rate of the bismuth (III) phosphinato-MFC sheets were measured at 23 ^{o}C and 50 % relative humidity by following ASTM E96, using the desiccant method (E96/E96M□16 2016). The sheets were pre-dried in an oven at 105 ^{o}C for at least four hours. Cups complying with the standard were filled with dried desiccant, calcium chloride, and sealed with the test sample. This arrangement was kept in the test condition chamber and the variation in mass of the permeability cups over time was recorded. The rate of change in mass quantifies the water vapour transmission rate (WVTR). The WVTR was then normalized by the thickness of the paper to determine water vapour permeability (WVP). The thickness of the composite sheets was measured using L&W thickness tester. A number of readings were taken for each sheet, and the mean thickness was calculated.

3. Results and Discussion

3.1. Characterisation

3.1.1. ICP-OES Analysis:

ICP-OES was used to quantify the actual amount of bismuth complex present in the sheets. Table 1 shows the mean percentage of bismuth complex to dry paper determined using ICP-OES analysis, along with the standard deviation (n=3). The results were found to be close to the expected values. However, the minor difference could be accounted for by loss of the complex while preparing the suspension or due to sticking of the complex within the spray system. The maximum loss (30%) was observed for 0.1wt%. loading which could mean that a larger proportion of the complex was lost on

the surfaces in contact with the suspension at low loadings than at high loadings of 5.0 wt.% (13% loss), with the 1.0 wt.% (6% loss) being an outlier. In this instance the preparation of the composites was done in small laboratory scale, with a much greater surface to volume ratio than would be the case in large scale production. When scaling this up to a large-scale production, these losses would be expected to be minimal.

Table 1: Percentage of phenyl bismuth bis(diphenylphosphinato) from ICP-OES analysis for the different loaded Bi-MFC composites

Target loading of bismuth complex wt. % (g bismuth complex/g cellulose)	Mean actual percentage of bismuth complex wt. % from ICP ± standard deviation (g bismuth complex/g dry paper)
0.1	0.07 ± 0.01
0.5	0.39 ± 0.05
1.0	0.94 ± 0.02
2.5	2.10 ± 0.05
5.0	4.37 ± 0.07

3.1.2. Bi-complex characterization

The bismuth(III) phosphinato complex precipitates from the reaction as long thin needles, as shown in the optical image of the bismuth complex alone in Figure S13. The particle size of the dispersed phase plays a significant role in the properties of composite materials. Due to the particles being non-spherical, light/laser scattering techniques do not define the actual dimensions of the particles. However, scattering techniques can be used to measure the hydrodynamic diameter of an equivalent sphere of the particle that has the same diffusion coefficient. The hydrodynamic diameter of the particle was found to be 1.25±0.18 µm, with a polydispersity index of 0.33±0.04. The complex is stable upto a temperature of 300 ^{o}C, found by TGA (Figure S12). The melting point and the decomposition point of the complex is 300 ^{o}C and 330 ^{o}C respectively and has been reported previously as well (Andrews, Werrett et al. 2018).

3.1.3. SEM Imaging

Scanning Electron Microscope (SEM) was used to study the distribution of the complex within the microfibrillated cellulose fibres. Secondary electron (SE) imaging was done to obtain surface information of the 4.37 wt.% Bi-MFC composite as shown in Figure 2. It is clear from the images that nanofibers form a highly entangled network, and the cylindrical inorganic complex particles are present on the surface entangled within the MFC fibres. It is evident that the particles vary in size and are arranged in random orientation with occasional clustering at different regions on the surface. The

dimensions of randomly selected particles on the surface were measured, and the particle size distribution is as illustrated in the Figure 3. The smallest particle was 525 nm, and the largest one detected was 13.3 µm.

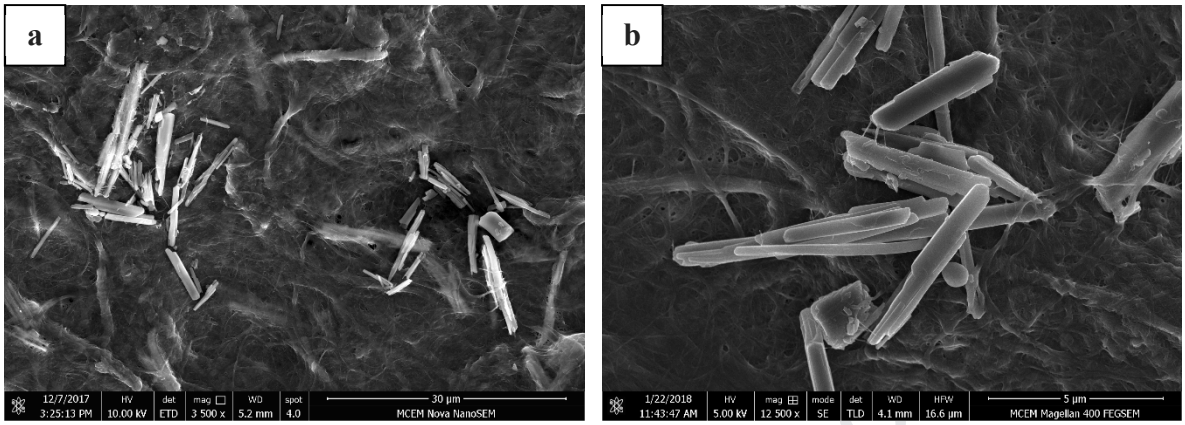

Figure 2: SEM images of the surface of 4.37 wt.% Bi-MFC composite at different magnifications: (a) ×3500 (b) ×12500

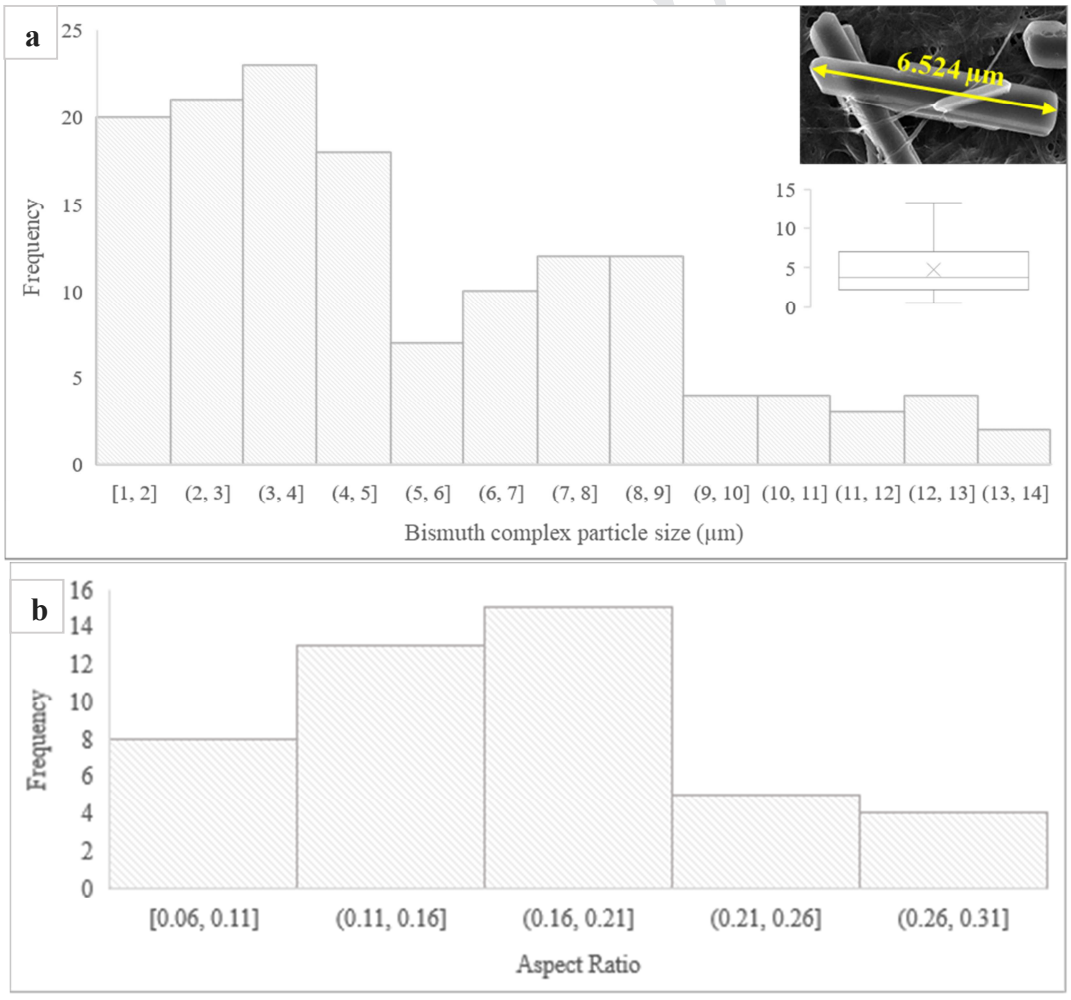

Figure 3 (a): Particle length distribution (n=140) and (b) Aspect ratio distribution (n=40) of bismuth (III) phosphinato complex on the surface of 4.37 wt.% Bi-MFC sheet

The shape of the particles can be observed to be cylindrical needle-shaped from Figure 2. For such a form, a simple parameter, aspect ratio, can be used to describe the shape. The aspect ratio, the ratio of the width to length of the particle, has been measured from SEM images and the aspect ratio distribution curve is shown in Figure 3(b). Figure 4 shows the secondary electron image and its corresponding energy-dispersive X-ray (EDX) mapping of the same bismuth (III) phosphinato-MFC composite. This, along with Figure S14 showing the EDX point analysis of the composite, confirms the presence of bismuth at the cylindrical needle-like structures. Moreover, it also shows that not only are the particles present on the surface, but that they are also buried inside the material (as indicated by arrows in Figure 4). This phenomenon of the particles being embedded deeper under the surface has also been supported by the back scattered electron images in Figure 5. The high atomic number of bismuth, compared to carbon, oxygen and hydrogen found in the cellulose, means that the bismuth complex appears much brighter in the BSE images. The bright needle-like structures in the BSE images indicate the presence of the bismuth (III) phosphinato complex. BSE imaging in Figure 5 was done in areas where not many cylindrical particles could be spotted with secondary electron imaging, but it was found that bismuth was present in those areas. A BSE image taken at low magnification, in Figure 6, shows that the bismuth (III) phosphinato structures can be seen throughout the space indicating that the inorganic complex is well distributed throughout the matrix.

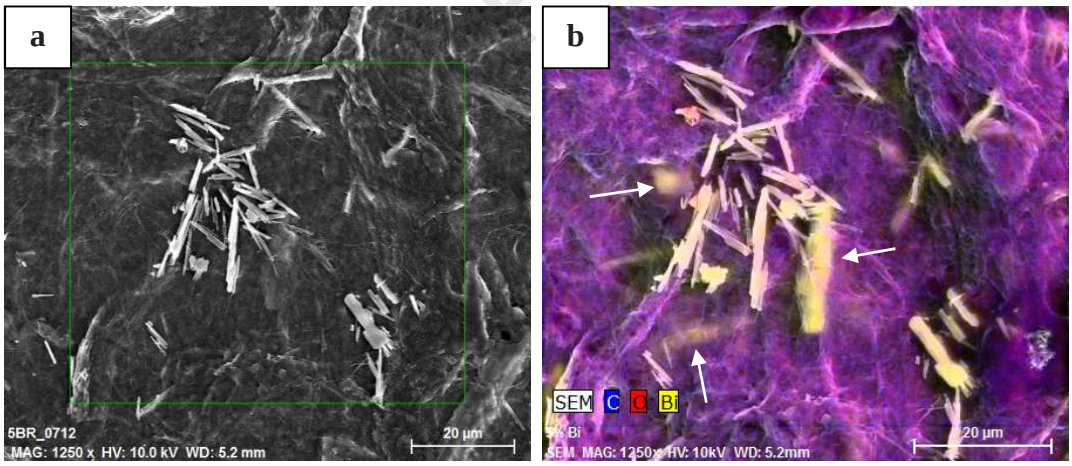

Figure 4: SEM images of the 4.37 wt.% Bi-MFC composite using (a) secondary electron imaging (b) EDX mapping of the selected area

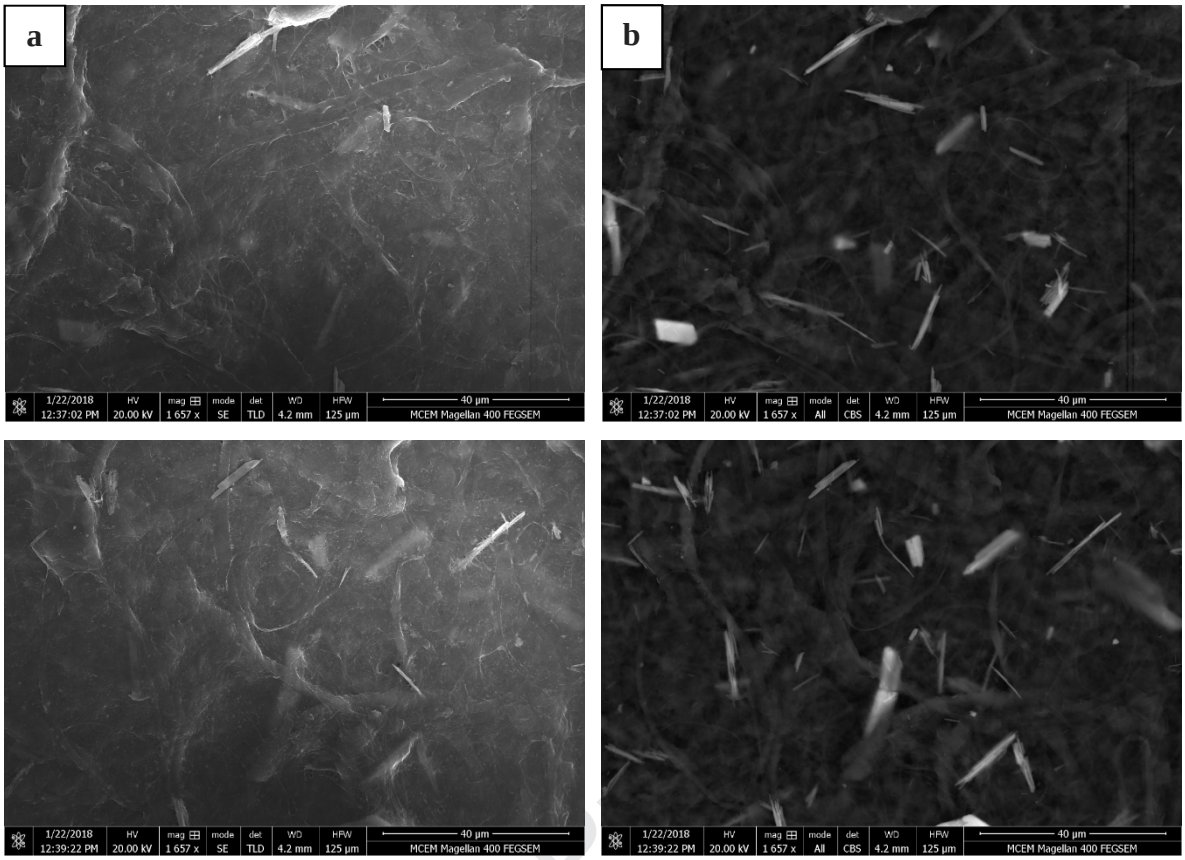

Figure 5: SEM images of the 4.37 wt.% Bi- MFC sheets using (a) secondary electron imaging and their corresponding (b) Back scattered electron imaging

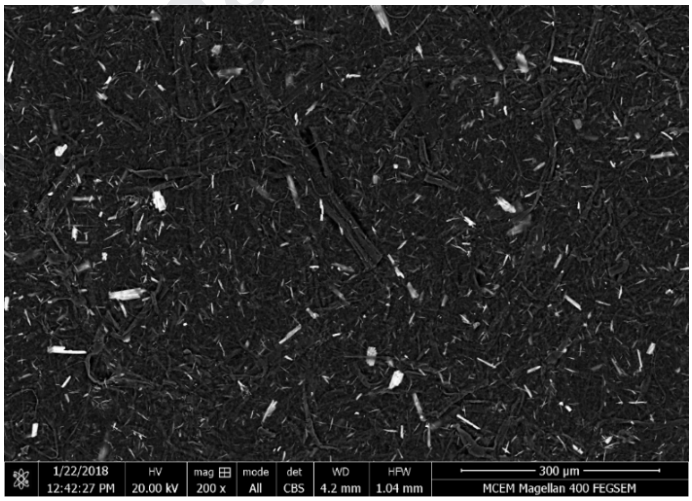

Figure 6: Back scattered electron image of the 4.37 wt.% Bi- MFC sheet at low magnification (×200)

Although the secondary images show some clustering of the complex, the BSE images and EDX mapping give clear evidence of the particles being buried under the surface and that there is an overall even distribution of the particles within the matrix. The fact that the particles are entrapped within the fibres also mean that the particles are well secured within the matrix, and this along with the insolubility of the complex should limit the release of bismuth out of the material, thereby minimizing the risks of environmental accumulation. Figure S15 shows the entanglement of the Bi-complex

within the nanocellulose fibres. This suggests that the bismuth complex is quite securely held within the composite structure.

3.2. Material performance

3.2.1. Antibacterial Activity

The disk diffusion assays show that sheets with higher bismuth complex loadings produce greater zones of inhibition. The agar plates for the zones of inhibition is shown in Figures S1 -S5 in the supplementary information and the results summarized in Figure 7. Figure 7 shows that the Gram-negative bacteria, *P. aeruginosa* and *E. coli*, are less susceptible to the Bi-MFC composite, as evidenced by smaller zones of inhibition compared to the Gram-positive bacteria. The composites provided little or no inhibition of Gram-negative bacteria at loadings below 0.94 wt.%. In contrast, Gram-positive bacteria showed evidence of growth inhibition even at the lowest levels of bismuth loading tested, which is 0.07 wt.%. These observations agree with previous work that showed that the bismuth (III) complex is more active against Gram-positive bacteria than Gram-negative strains (Kotani, Nagai et al. 2005, Luqman, Blair et al. 2016, Andrews, Werrett et al. 2018). Gram-negative bacteria are in general harder to kill or inhibit as these cells are surrounded by an outer membrane of lipopolysaccharide, which is absent in Gram-positive bacteria. This extra outer membrane in Gram-negative bacteria acts as a permeability barrier to antibiotics and bactericidal agents making attack more difficult (Tegos, Stermitz et al. 2002). Figure 7 also shows that the increase in effectiveness with increased loadings becomes less pronounced for higher loadings and the antibacterial activity seems to reach a plateau beyond 2.10 wt. %, as observed by the trends for *E. coli, P. aeruginosa* and MRSA.

The results also showed the bismuth-loaded composites were as effective against the drug-resistant form of *S. aureus*, i.e. MRSA as it was to the more sensitive strain of this medically-important bacterium. MRSA is very difficult to treat by most antibiotics and is a major problem in the hospital system (Patra, Gasser et al. 2012). Silver-resistance has been reported in 33 strains of MRSA (Loh, Percival et al. 2009). We examined a limited set of MRSA strains in this study but it raises the possibility that these bismuth-based materials could potentially replace silver-based ones. Based on the results, it was demonstrated that bismuth (III) phosphinato loaded sheets are active against the Gram-positive bacteria and to a lesser extent the Gram-negative bacteria.

Previous research showed bacterial nanocellulose- silver nanoparticle composite with 1.01 wt% loading produced small zones of inhibition against *E. coli*, *S. aureus* and *P. aeruginosa*, with all results being below 8mm (Wu, Zheng et al. 2014). When compared to bismuth composites, with a similar loading of 0.94 wt.%, the zones of inhibitions were 8.7 mm, 17 mm and 7 mm respectively. Also, it was reported that silver sulfadiazine loaded nanocellulose sheets with 0.43 wt.% loading produced a 9 mm zone of inhibition against VRE (Andrews, Werrett et al. 2018). Whereas in Figure 7, we can observe that bismuth composites with a much lower loading of 0.072 wt.% produced an 8

mm diameter zone of inhibition diameter against the same bacteria. Based on the zones of inhibition, it can be inferred that the bismuth loaded nanocellulose composites have an equal or greater activity than similar composites loaded with silver-based antibacterial agents.

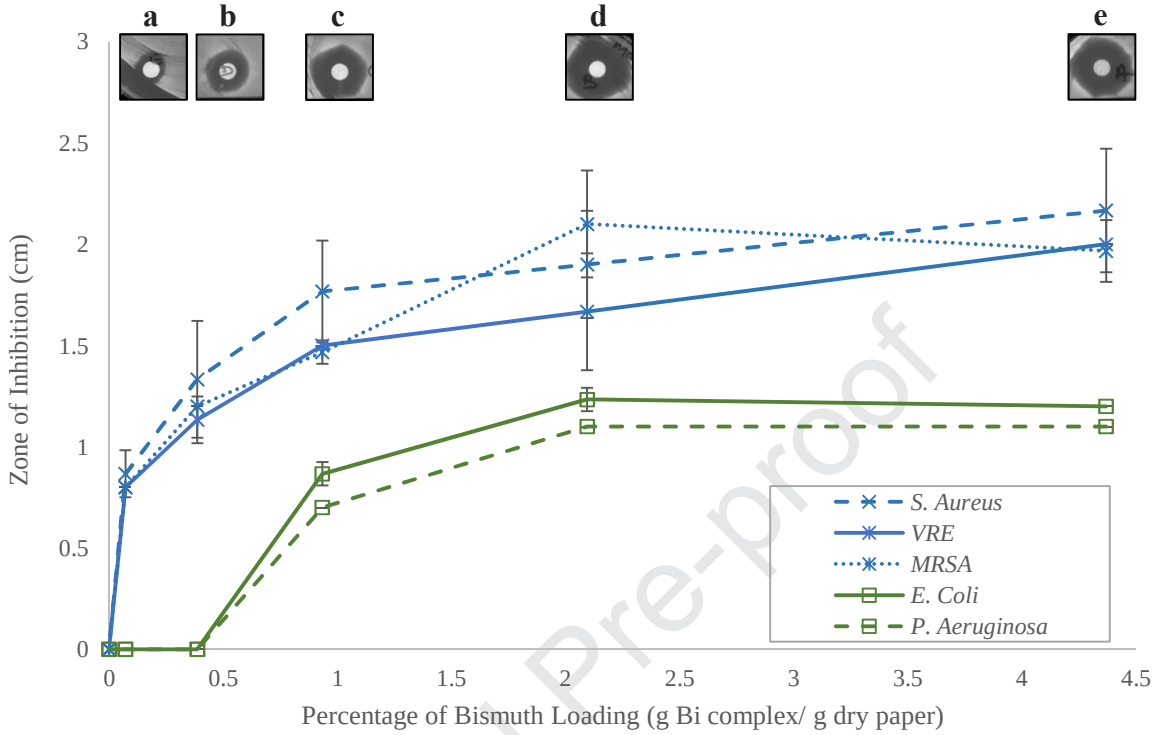

Figure 7: Effect of bismuth complex loading on zone of inhibition with different bacteria from disk diffusion assay and the top images show their picture representation against S. aureus

3.2.2. Antifungal Activity

It was found that the bismuth (III) phosphinato loaded composites were effective against several fungi species, including the pathogenic *C. glabrata* and *C. albicans*. The zone of inhibition on the fungal plates were similar in size to that observed for *P. aeruginosa* and *E.coli*, suggesting a lower level of inhibition but one that may still prove useful to control contamination of products inside the packaging. Table 2 shows the zones of inhibition of the composites against fungal species. Some of the fungal species were hard to grow evenly across the plate, which made visual assessment difficult, as shown in Figures S6-S9 in the supplementary information. However, close examination and measurement of the halo allowed an objective comparison of the effect of the composite on all of the yeasts. Since the results for *C. glabrata* were inconclusive for all samples tested, further experiments were done with a higher composite loading of 10.53 wt.% and a zone in the range 0.6 cm to 0.8 cm was observed. On the other hand, for *C. albicans*, a zone of inhibition was observed even at the low loading of 0.94 wt.%. Overall, this composite is shown to be effective not only on bacteria but also on some pathogenic fungi strains.

Table 2: Antifungal activity of the Bi-MFC composites determined by the zone of inhibition assay

	Percentage of bismuth loading (g Bi complex/ g dry paper)						
Test Fungus	0	0.07	0.39	0.94	2.01	4.37	10.53
S. pombe	−	−	−	±	±	+	++
S. cerevisiae	−	−	−	+	++	++	++
C. glabrata	−	−	−	±	±	±	+
C. albicans	−	−	−	+	++	++	++

− no inhibition

± not clear/ inconclusive

\+ clear zone of 0.6-0.8 cm

++ clear zone greater than 0.8 cm

3.2.3. Duration of antimicrobial action

It was observed that the activity of the bismuth(III) phosphinato-MFC composites decreased with time for both samples, illustrated by the decreasing zone of inhibition with time in Figure 8(a) and Figure S10, which was performed in triplicates. The 0.94 wt.% and 4.37 wt.% loaded sheets remained active for 3 and 5 days respectively. Also, the zone of inhibition was greater for the 4.37 wt.% sheets at all times due to presence of higher amounts of active complex.

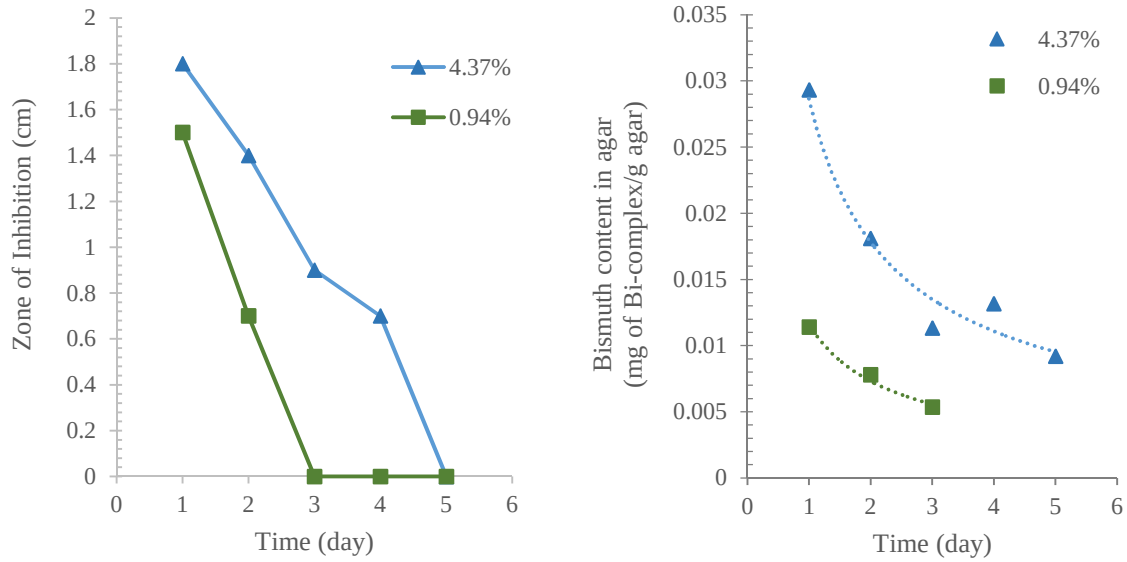

Figure 8: Zone of inhibition (a) and the amount of bismuth content leached out into the zone of inhibition (b) for the 4.37 wt.% and 0.94 wt.% loaded bismuth sheets with time

exhausted composites were further analysed by ICP-OES, and the final bismuth content was found to be 0.15 wt.% and 0.04 wt.% (g of Bi-complex/g dry paper) for the 4.37 wt% and 0.94 wt.% original composites respectively after 5 days of agar testing. Thus, the complex will eventually leach out of the composite to work on the bacteria when in contact with it, but remains securely held within the fibres while being transported or handled.

3.2.4. Physical and Mechanical properties

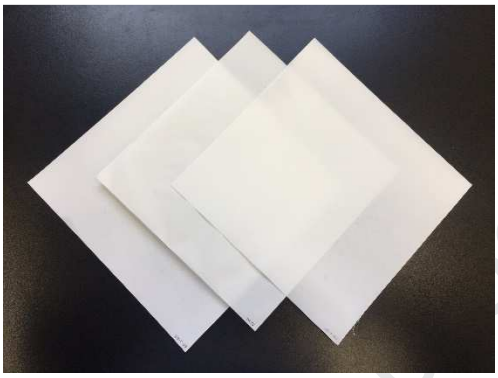

Figure 9: Physical appearance of the 0.39 wt.%, 0.94 wt.% and 2.10 wt.% bismuth (III) phosphinato-MFC sheets (left to right)

The pure MFC sheet and all the composites are white and opaque, with no visible difference among them to the naked eye. The sheets are satisfactorily homogenous in terms of thickness and basis weight, as reported in Table S2 in the supplementary information. It was observed that the addition of the Bi-complex into MFC affects the mechanical strength of the sheets formed. The tensile index for the pure MFC sheet was found to be 76.5±5.8 Nm/g. However, with only 0.07 wt.% Bi-complex additive added to the composite, the tensile index dropped to 55.8±1.0 Nm/g. On a higher loading of 4.37 wt.%, the tensile index further dropped to 40.0±1.5 Nm/g. These values are comparable to the mechanical strength of similar MFC sheets, which were reported to be in the range 45-104 Nm/g (Beneventi, Zeno et al. 2016). Similar trends were observed for the Young's modulus, which were 8.4±0.4 GPa, 7.6±0.3 GPa and 5.4±0.3 GPa for 0 wt.%, 0.07 wt.% and 4.37 wt.% Bi-loaded composites, respectively. The Young's modulus of pure MFC has been reported by various researchers to be up to 6 GPa (Gabr, Phong et al. 2013). It can be suggested that the Bi-complex particles interferes with the inter-fibre bonding, which has been recognised to directly impact the mechanical properties of such composites (Sehaqui, Liu et al. 2010). At higher loadings, any agglomerated hydrophobic cluster can thus result in poor bonding between the cellulose chains. A similar effect was reported for high loading of nanoclay in MFC composites (Gabr, Phong et al. 2013, Garusinghe, Varanasi et al. 2018).

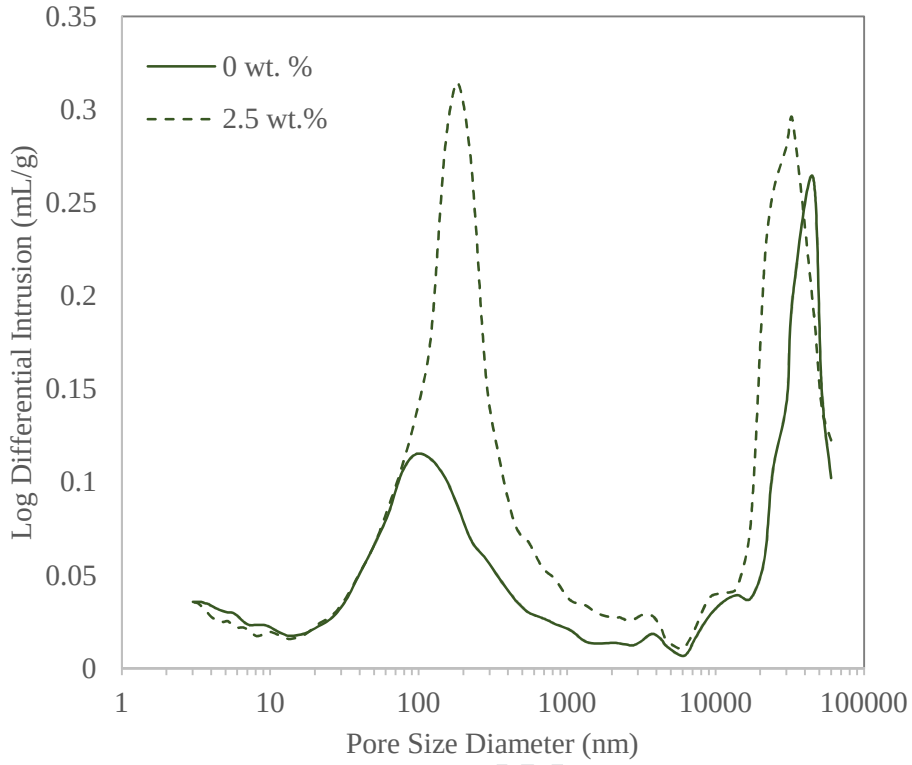

Figure 10: Pore size distribution for pure MFC sheet and Bi-MFC composite

The pore structure analysis was done, where the 2.10 wt.% Bi-MFC composite was chosen as it was the closest to the pure MFC sheet in terms of grammage. Figure 10 shows bimodal distribution of pore size in both the pure MFC sheet and the Bi-MFC composite. The modal pore size range did not seem to change much with the addition of bismuth complex. However, there seems to be significantly higher number of smaller pores as well as slightly more larger pores for the Bi-loaded composite than the pure MFC sheet, hence also explaining the rise in overall porosity reported in Table 4. The increased number of pores, along with the added surface from the bismuth particles, explains the rise in BET surface area for the Bi-MFC composite as reported in Table 4. The shape of the adsorption-desorption isotherm obtained from physisorption of nitrogen, in Figure S16, also tells us the material has slit-shaped pores, rather than cylindrical ones, according to the IUPAC classification of porous materials (Alothman 2012).

Table 4: Pore properties of the pure MFC sheet and Bi-MFC composite

Property	Pure MFC	2.10 wt. % Bi-MFC composite
Porosity (%)	19.3	28.9
Total intrusion volume (mL/g)	0.2357	0.3678
BET surface area (m^2/g)	0.4112 ± 0.0011	0.7552 ± 0.0020

3.2.5. Water vapour permeability

Packaging materials must be able to act as a barrier to the entry of water vapour in order to protect packaged goods from contamination and degradation. Molecule migration across a polymer film depends on the adsorption and desorption ability of the molecule on the surface and particularly on the rate of molecule diffusion across the film (Nair, Zhu et al. 2014). The dense network of the microfibrillated cellulose fibres creates small pores across the surface of the MFC sheets and increases the mean free path that the water molecule has to travel to reach the other end, i.e. it increases the tortuosity of travel as compared to normal cellulose.

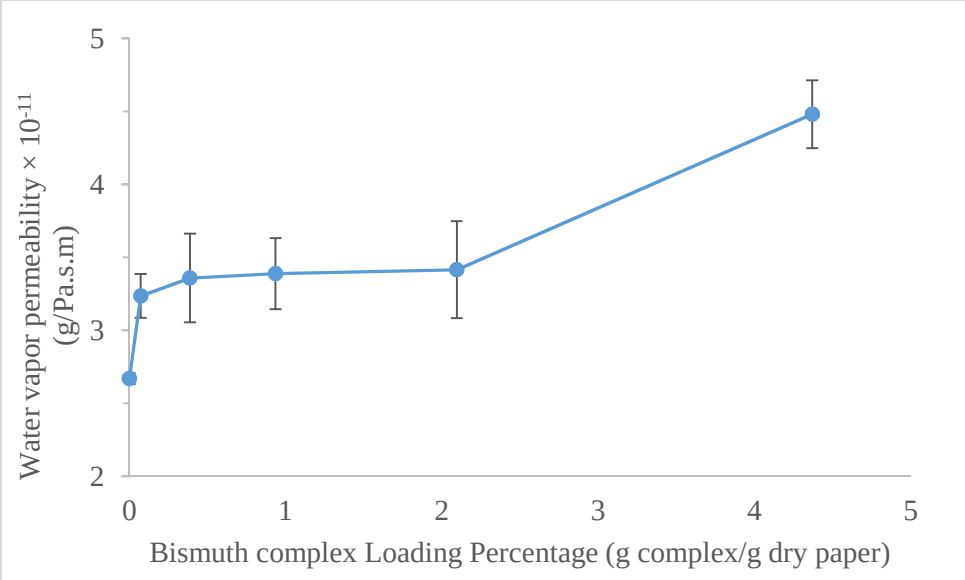

Figure 11: Effect of bismuth complex loading on the water vapour permeability of the phenyl bismuth bis(diphenylphosphinato) functionalized MFC

However, with addition of the bismuth complex, the WVP was observed to increase slightly as shown in Figure 11. The SEM images and EDX mapping confirmed the even distribution of the complex throughout the material, with evidence of them being distributed under the surface. It was also observed that the particles were large, with the largest observed dimension of 13 microns. It can be proposed that arrangement of some of the particles with its largest dimension parallel to the diffusion pathway allowed water vapour molecules to follow a more direct path rather than a tortuous path. This resulted in minor reductions in the WVP performance. Increasing the loading from 0.07 wt.% to 2.10 wt. % did not significantly alter WVP performance. Surprisingly, increasing the loading to 4.37 wt.% showed a sudden increase. It can be proposed that after a certain loading, the complex becomes interconnected due to aggregation of the hydrophobic complexes. It is possible that at this point the percolation threshold might have been reached, creating a conducting pathway that increases the WVP. It has been reported that diffusion across a material with embedded tubular particles increases with an increase in concentration of the particles within, and the most significant change occurs near the percolation threshold (Grekhov, Eremin et al. 2013, Likhomanova, Tronin et al. 2015). The barrier

properties are dependent on a number of factors, which include the size and shape of the additive agent, its distribution as well as the total amount present in the structure (Garusinghe, Varanasi et al. 2018). All these parameters have been studied to support the hypothesis. However, the effect of the complex was very minor and was still in the range of 10^{-11} when compared to the WVP of commercial plastic based packaging materials, which are within 10^{-12} to 10^{-13} range (Aulin and Lindstrom , Bourlieu, Guillard et al. 2009).

Table 3: Literature comparison of WVP of common packaging materials with Bi-MFC composites

Film	WVP $\times 10^{-11}$ (g/m.Pa.s)	Relative Humidity (%)	Temperature (^{o}C)	Reference
Experimental sheets				
Pure MFC sheet	2.67	0-50%	23	-
Bi-MFC composites	3.23-4.48	0-50%	23	-
Synthetic Films				
HDPE	0.002	0-100	27.6	(Bourlieu, Guillard et al. 2009)
LDPE	0.014	-	27.6	
PP	0.010	-	25	
PVC	0.041		27.6	
PSs	0.5	0-100	25	(Aulin and Lindstrom)
Biobased Films				
Cellulose derivatives	9.2-11	0-85%	21	(Park and Chinnan 1995)
Chitosan	13	76.2	25	(Rhim and Ng 2007)

Table 3 compares the values of WVP for various packaging materials. The published data were obtained using different testing conditions and so are not exactly comparable to our values without considering the relative humidity and temperature. A higher relative humidity gives higher permeability values for a test sample. However, these values provide an indication of the Bi-MFC sheets performance with respect to commercial packaging materials. The WVP values of the bismuth-based sheets are not as low as those for synthetic films, but further modifications may be possible to arrive at similar performance levels. Additionally, of course, the bismuth-impregnated material has the advantage of being antimicrobial against some of the medically important microorganisms. However, to be used as a packaging material for food packaging applications in particular, further investigation with food pathogens will be required. Moreover, the antimicrobial additive will get used up during its application, thereby losing its effectiveness over time and ensuring that the material is

recyclable and biodegradable. The biodegradability and renewability of nanocellulose further makes this material a sustainable and eco-friendly product that not only safeguards public health but also protects the environment throughout its life cycle.

This material can be the answer to a number of environmental issues from a broad cleaner production perception that has the antimicrobial and barrier properties for use as a packaging material along with

- being a safer alternative to silver-based material, addressing all the issues of overuse of silver, viz. environmental accumulation, cytotoxicity and induction of resistance in bacteria
- using a biodegradable and renewable natural polymer as the matrix

4. Conclusion

The study investigated the preparation of bismuth-based nanocellulose composites on an industrial scale using a spraying system for the development of a biodegradable and renewable active packaging material. The composites prepared in this study have antimicrobial properties against some of the most medically-important bacteria and fungi, along with the virtue of having activity at relatively low loadings. There is a clear dose effect on the performance of these sheets. In addition, the composites have reasonable barrier performance against water vapour, with the bismuth complex not having any significant effect on the barrier performance unless present at relatively high levels. The physical and mechanical properties are also affected by the addition of the complex, but were still in expected range within the scope of study. Bismuth-based nanocellulose composites have potential to serve as a cleaner antimicrobial barrier material and can potentially replace silver-based packaging material. However, a proper understanding of the loading and its corresponding material properties needs to be fully understood, and this paper provides a fair direction for doing so.

5. Acknowledgements

We would like to thank Kirubanandan Shanmugam (BioPRIA) for assistance with sheet preparation. The authors thank Monash University and The National Health and Medical Research Council (APP1139844) for financial support. The authors would like to acknowledge the use of the facilities in the Monash Centre for Electron Microscopy. Maisha Maliha and Megan Herdman would like to acknowledge the Australian Government for the Research Training Program (RTP) Scholarship.

References

Abd-El-Aziz, A. S., C. Agatemor and N. Etkin (2017). "Antimicrobial resistance challenged with metal-based antimicrobial macromolecules." Biomaterials 118: 27-50.

Alothman, Z. (2012). "A Review: Fundamental Aspects of Silicate Mesoporous Materials." Materials 5(12): 2874-2902.

Alvarez-Paino, M., A. Munoz-Bonilla and M. Fernandez-Garcia (2017). "Antimicrobial Polymers in the Nano-World." Nanomaterials (Basel) 7(2).

Amini, E., M. Azadfallah, M. Layeghi and R. Talaei-Hassanloui (2016). "Silver-nanoparticle-impregnated cellulose nanofiber coating for packaging paper." Cellulose 23(1): 557-570.

Andrews, P. C., M. Werrett, M. Herdman, R. Brammananth, U. Garusinghe, W. Batchelor, P. Crellin and R. Coppel (2018). "Bismuth Phosphinates in Bi-Nanocellulose Composites and their Efficacy towards Multi-Drug Resistant Bacteria." Chemistry (Weinheim an der Bergstrasse, Germany).

Appendini, P. and J. H. Hotchkiss (2002). "Review of antimicrobial food packaging." Innovative Food Science & Emerging Technologies 3(2): 113-126.

Aulin, C. and T. Lindstrom Biopolymer Coatings for Paper and Paperboard. Biopolymers – New Materials for Sustainable Films and Coatings.

Barros-Velázquez, J. Industrial Applications: Regulatory Issues and Life Cycle Assessment of Food Packaging. Antimicrobial Food Packaging, Elsevier.

Barry, N. P. E. and P. J. Sadler (2013). "Exploration of the medical periodic table: towards new targets." Chem. Commun. 49(45): 5106-5131.

Beneventi, D., D. Chaussy, D. Curtil, L. Zolin, C. Gerbaldi and N. Penazzi (2014). "Highly Porous Paper Loading with Microfibrillated Cellulose by Spray Coating on Wet Substrates." Industrial & Engineering Chemistry Research 53(27): 10982-10989.

Beneventi, D., E. Zeno and D. Chaussy (2016). "Rapid nanopaper production by spray deposition of concentrated microfibrillated cellulose slurries." ATIP. Association Technique de L'Industrie Papetiere 70(2): 6-14.

Bourlieu, C., V. Guillard, B. Vallès-Pamiès, S. Guilbert and N. Gontard (2009). "Edible Moisture Barriers: How to Assess of their Potential and Limits in Food Products Shelf-Life Extension?" Critical Reviews in Food Science and Nutrition 49(5): 474-499.

Briand, G. G. and N. Burford (1999). "Bismuth Compounds and Preparations with Biological or Medicinal Relevance." Chemical Reviews 99(9): 2601-2658.

Cao, H. (2017). Silver nanoparticles for antibacterial devices : biocompatibility and toxicity, Boca Raton : CRC Press, Taylor & Francis Group.

Carbone, M., D. T. Donia, G. Sabbatella and R. Antiochia (2016). "Silver nanoparticles in polymeric matrices for fresh food packaging." Journal of King Saud University - Science 28(4): 273-279.

Crocetti, G. (2013). "Save the nano-silver for where it's needed." Chain Reaction(117): 16.

Cushen, M., J. Kerry, M. Morris, M. Cruz-Romero and E. Cummins (2012). "Nanotechnologies in the food industry – Recent developments, risks and regulation." Trends in Food Science & Technology 24(1): 30-46.

Dankovich, T. A. and D. G. Gray (2011). "Bactericidal paper impregnated with silver nanoparticles for point-of-use water treatment." Environ Sci Technol 45(5): 1992-1998.

Dizaj, S. M., F. Lotfipour, M. Barzegar-Jalali, M. H. Zarrintan and K. Adibkia (2014). "Antimicrobial activity of the metals and metal oxide nanoparticles." Materials Science and Engineering: C 44: 278-284.

Domenico, P., L. Baldassarri, P. E. Schoch, K. Kaehler, M. Sasatsu and B. A. Cunha (2001). "Activities of Bismuth Thiols against Staphylococci and Staphylococcal Biofilms." Antimicrobial Agents and Chemotherapy 45(5): 1417.

Drake, P. L. and K. J. Hazelwood (2005). "Exposure-related health effects of silver and silver compounds: a review." Ann Occup Hyg 49(7): 575-585.

E96/E96M□16, A. (2016). Standard Test Methods for Water Vapor Transmission of Materials, ASTM International West Conshohocken, PA.

Echegoyen, Y. and C. Nerín (2013). "Nanoparticle release from nano-silver antimicrobial food containers." Food and Chemical Toxicology 62: 16-22.

Fey, P. D. and M. E. Olson (2010). "Current concepts in biofilm formation of Staphylococcus epidermidis." Future microbiology 5(6): 917-933.

Fidel, P. L., Jr., J. A. Vazquez and J. D. Sobel (1999). "Candida glabrata: review of epidemiology, pathogenesis, and clinical disease with comparison to C. albicans." Clin Microbiol Rev 12(1): 80-96.

Gabr, M. H., N. T. Phong, M. A. Abdelkareem, K. Okubo, K. Uzawa, I. Kimpara and T. Fujii (2013). "Mechanical, thermal, and moisture absorption properties of nano-clay reinforced nano-cellulose biocomposites." Cellulose 20(2): 819-826.

Garusinghe, U. M., S. Varanasi, V. S. Raghuwanshi, G. Garnier and W. Batchelor (2018). "Nanocellulose-montmorillonite composites of low water vapour permeability." Colloids and Surfaces A: Physicochemical and Engineering Aspects 540: 233-241.

Grekhov, A. M., Y. S. Eremin, G. A. Dibrov and V. V. Volkov (2013). "Percolation of composite poly(vinyltrimethylsilane) membranes with carbon nanotubes." Petroleum Chemistry 53(8): 549-553.

Gunawan, C., C. P. Marquis, R. Amal, G. A. Sotiriou, S. A. Rice and E. J. Harry (2017). "Widespread and Indiscriminate Nanosilver Use: Genuine Potential for Microbial Resistance." ACS nano 11(4): 3438.

Haider, A. and I. K. Kang (2015). "Preparation of Silver Nanoparticles and Their Industrial and Biomedical Applications: A Comprehensive Review." Advances in Materials Science and Engineering 2015: 1-16.

Hua, X., X. Yuan, B. M. Mitchell, M. C. Lorenz, D. M. O'Day and K. R. Wilhelmus (2009). "Morphogenic and genetic differences between Candida albicans strains are associated with keratomycosis virulence." Mol Vis 15: 1476-1484.

Huang, J.-Y., X. Li and W. Zhou (2015). "Safety assessment of nanocomposite for food packaging application." Trends in Food Science & Technology 45(2): 187-199.

Huang, Y., S. Chen, X. Bing, C. Gao, T. Wang and B. Yuan (2011). "Nanosilver Migrated into Food-Simulating Solutions from Commercially Available Food Fresh Containers." Packaging Technology and Science 24(5): 291-297.

Inamuddin (2016). Green Polymer Composites Technology : Properties and Applications. Boca Raton, UNITED KINGDOM, Chapman and Hall/CRC.

Kawashima, S. A., A. Takemoto, P. Nurse and T. M. Kapoor (2012). "Analyzing fission yeast multidrug resistance mechanisms to develop a genetically tractable model system for chemical biology." Chem Biol 19(7): 893-901.

Keogan, D. and D. Griffith (2014). "Current and Potential Applications of Bismuth-Based Drugs." Molecules 19(9): 15258.

Klemm, D., B. Heublein, H.-P. Fink and A. Bohn (2005). "Cellulose: Fascinating Biopolymer and Sustainable Raw Material." Angewandte Chemie International Edition 44(22): 3358-3393.

Klemm, D., F. Kramer, S. Moritz, T. Lindström, M. Ankerfors, D. Gray and A. Dorris (2011). "Nanocelluloses: A New Family of Nature-Based Materials." Angewandte Chemie International Edition 50(24): 5438-5466.

Kotani, T., D. Nagai, K. Asahi, H. Suzuki, F. Yamao, N. Kataoka and T. Yagura (2005). "Antibacterial Properties of Some Cyclic Organobismuth(III) Compounds." Antimicrobial Agents and Chemotherapy 49(7): 2729.

Krol, L. F., D. Beneventi, F. Alloin and D. Chaussy (2015). "Microfibrillated cellulose-SiO2 composite nanopapers produced by spray deposition." Journal of Materials Science 50(11): 4095-4103.

Kumar, V., R. Bollström, A. Yang, Q. Chen, G. Chen, P. Salminen, D. Bousfield and M. Toivakka (2014). "Comparison of nano- and microfibrillated cellulose films." Cellulose 21(5): 3443-3456.

Kumar, V., V. R. Koppolu, D. Bousfield and M. Toivakka (2017). "Substrate role in coating of microfibrillated cellulose suspensions." Cellulose 24(3): 1247-1260.

Lavoine, N., I. Desloges, A. Dufresne and J. Bras (2012). "Microfibrillated cellulose - its barrier properties and applications in cellulosic materials: a review." Carbohydr Polym 90(2): 735-764.

Lavoine, N., I. Desloges, B. Manship and J. Bras (2015). "Antibacterial paperboard packaging using microfibrillated cellulose." J Food Sci Technol 52(9): 5590-5600.

Lavoine, N., V. Guillard, I. Desloges, N. Gontard and J. Bras (2016). "Active bio-based food-packaging: Diffusion and release of active substances through and from cellulose nanofiber coating toward food-packaging design." Carbohydr Polym 149: 40-50.

Lemire, J. A., J. J. Harrison and R. J. Turner (2013). "Antimicrobial activity of metals: mechanisms, molecular targets and applications." Nature Reviews Microbiology 11: 371.

Likhomanova, P. A., I. V. Tronin, A. M. Grekhov and Y. S. Eremin (2015). "Modeling of Particle Diffusion in Heterogeneous Structure Near to the Percolation Threshold." Physics Procedia 72: 42-46.

Lin, N. and A. Dufresne (2014). "Nanocellulose in biomedicine: Current status and future prospect." Eur. Polym. J. 59: 302-325.

Loh, J. V., S. L. Percival, E. J. Woods, N. J. Williams and C. A. Cochrane (2009). "Silver resistance in MRSA isolated from wound and nasal sources in humans and animals." International Wound Journal 6(1): 32-38.

Luqman, A., V. L. Blair, R. Brammananth, P. K. Crellin, R. L. Coppel and P. C. Andrews (2016). "The Importance of Heterolepticity in Improving the Antibacterial Activity of Bismuth(III) Thiolates." European Journal of Inorganic Chemistry 2016(17): 2738-2749.

Maillard, J.-Y. and P. Hartemann (2013). "Silver as an antimicrobial: facts and gaps in knowledge." Critical Reviews in Microbiology 39(4): 373-383.

Martínez-Abad, A., J. M. Lagaron and M. J. Ocio (2012). "Development and Characterization of Silver-Based Antimicrobial Ethylene–Vinyl Alcohol Copolymer (EVOH) Films for Food-Packaging Applications." Journal of Agricultural and Food Chemistry 60(21): 5350-5359.

Nair, S. S., J. Zhu, Y. Deng and A. J. Ragauskas (2014). "High performance green barriers based on nanocellulose." Sustainable Chemical Processes 2(1): 23.

O'Sullivan, A. C. (1997). "Cellulose: the structure slowly unravels." Cellulose 4(3): 173-207.

Pal, C., J. Bengtsson-Palme, C. Rensing, E. Kristiansson and D. G. J. Larsson (2014). "BacMet: antibacterial biocide and metal resistance genes database." Nucleic acids research 42(Database issue): D737.

Park, H. J. and M. S. Chinnan (1995). "Gas and water vapor barrier properties of edible films from protein and cellulosic materials." Journal of Food Engineering 25(4): 497-507.

Patra, M., G. Gasser and N. Metzler-Nolte (2012). "Small organometallic compounds as antibacterial agents." Dalton Transactions 41(21): 6350-6358.

Pereira De Abreu, D. A., J. M. Cruz and P. Paseiro Losada (2012). "Active and Intelligent Packaging for the Food Industry." Food Reviews International 28(2): 146-187.

Pezzuto, A., C. Losasso, M. Mancin, F. Gallocchio, A. Piovesana, G. Binato, A. Gallina, A. Marangon, R. Mioni, M. Favretti and A. Ricci (2015). "Food safety concerns deriving from the use of silver based food packaging materials." Frontiers in microbiology 6: 1109-1109.

Rhim, J.-W. and P. K. W. Ng (2007). "Natural Biopolymer-Based Nanocomposite Films for Packaging Applications." Critical Reviews in Food Science and Nutrition 47(4): 411-433.

Sehaqui, H., A. Liu, Q. Zhou and L. A. Berglund (2010). "Fast preparation procedure for large, flat cellulose and cellulose/inorganic nanopaper structures." Biomacromolecules 11(9): 2195-2198.

Shanmugam, K., S. Varanasi, G. Garnier and W. Batchelor (2017). "Rapid preparation of smooth nanocellulose films using spray coating.(Report)(Author abstract)." Cellulose 24(7): 2669.

Silver, S. (2003). "Bacterial silver resistance: molecular biology and uses and misuses of silver compounds." FEMS Microbiology Reviews 27(2): 341-353.

Siró, I. and D. Plackett (2010). "Microfibrillated cellulose and new nanocomposite materials: a review." Cellulose 17(3): 459-494.

Stensberg, M. C., Q. Wei, E. S. McLamore, D. M. Porterfield, A. Wei and M. S. Sepulveda (2011). "Toxicological studies on silver nanoparticles: challenges and opportunities in assessment, monitoring and imaging." Nanomedicine (Lond) 6(5): 879-898.

Suzuki, H. and Y. Matano (2001). Chapter 1 - Introduction A2 - Suzuki, Hitomi. Organobismuth Chemistry. Y. Matano. Amsterdam, Elsevier Science: 1-20.

Svoboda, T., R. Jambor, A. Ruzicka, Z. Padelkova, M. Erben and L. Dostal (2010). "NCN Chelated Organoantimony(III) and Organobismuth(III) Phosphinates and Phosphites: Synthesis, Structure and Reactivity." European Journal of Inorganic Chemistry 2010(33): 5222-5230.

Tegos, G., F. R. Stermitz, O. Lomovskaya and K. Lewis (2002). "Multidrug Pump Inhibitors Uncover Remarkable Activity of Plant Antimicrobials." Antimicrobial Agents and Chemotherapy 46(10): 3133.

Varanasi, S. and W. J. Batchelor (2013). "Rapid preparation of cellulose nanofibre sheet." Cellulose 20(1): 211-215.

Varanasi, S., H. Chiam and W. Batchelor (2012). "Application and interpretation of zero and short-span testing on nanofibre sheet materials." Nord. Pulp Paper Res. J. 27(2): 343-351.

Wu, J., Y. Zheng, W. Song, J. Luan, X. Wen, Z. Wu, X. Chen, Q. Wang and S. Guo (2014). "In situ synthesis of silver-nanoparticles/bacterial cellulose composites for slow-released antimicrobial wound dressing." Carbohydrate Polymers 102: 762.

Xiong, Z. C., Y. J. Zhu, F. F. Chen, T. W. Sun and Y. Q. Shen (2016). "One-Step Synthesis of Silver Nanoparticle-Decorated Hydroxyapatite Nanowires for the Construction of Highly Flexible Free-Standing Paper with High Antibacterial Activity." Chemistry 22(32): 11224-11231.

Xu, Q., C. Chen, K. Rosswurm, T. Yao and S. Janaswamy (2016). "A facile route to prepare cellulose-based films." Carbohydrate Polymers 149: 274-281.

Yan, J., A. M. Abdelgawad, M. E. El-Naggar and O. J. Rojas (2016). "Antibacterial activity of silver nanoparticles synthesized In-situ by solution spraying onto cellulose." Carbohydr Polym 147: 500-508.